J.Cell.Mol.Med. Vol 6, No 1, 2002 pp. 82-92

Kinetics of apoptotic markers in exogeneously induced apoptosis of EL4 cells

Robert Jessel [a], Steffen Haertel [a], Carmen Socaciu [b] *, Svetlana Tykhonova [a], Horst A. Diehl [a]

[a] *Biophysical Department, Institute of Experimental Physics, University of Bremen, Bremen, Germany*

[b] *Department of Chemistry and Biochemistry, University of Agricultural Sciences and Veterinary Medicine, Cluj-Napoca, Romania*

Received: March 1, 2002; Accepted: March 22, 2002

Abstract

We investigated the time-dependence of apoptotic events in EL4 cells by monitoring plasma membrane changes in correlation to DNA fragmentation and cell shrinkage. We applied three apoptosis inducers (staurosporine, tubericidine and X-rays) and we looked at various markers to follow the early-to-late apoptotic events: phospholipid translocation (identified through annexin V-fluorescein assay and propidium iodide), lipid package (via merocyanine assay), membrane fluidity and anisotropy (via fluorescent measurements), DNA fragmentation by the fluorescence-labeling test and cell size measurements. The different apoptotic inducers caused different reactions of the cells: staurosporine induced apoptosis most rapidly in a high number of cells, tubercidine triggered apoptosis only in the S phase cells, while X-rays caused a G2/M arrest and subsequently apoptosis. Loss of lipid asymmetry is promptly detectable after one hour of incubation time. The phosphatidylserine translocation, decrease of lipid package and anisotropy, and the increase of membrane fluidity appeared to be based on the same process of lipid asymmetry loss. Therefore, the DNA fragmentation and the cell shrinkage appear to be parallel and independent processes running on different time scales but which are kinetically inter-related. The results indicate different signal steps to apoptosis dependent on inducer characteristics but the kinetics of "early-to-late" apoptosis appears to be a fixed program.

Keywords: EL4 cells - apoptosis - staurosporine - tubercidine - x-rays - phospholipid translocation - lipid package - membrane anisotropy - DNA fragmentation - DAPI test

Introduction

Apoptosis pathways are genetically determined. They involve physiological mechanisms of cell death in order to eliminate aberrant cells. During apoptosis, characteristic changes of cell structure occur, such as cell shrinking, membrane blebbings, changes of the plasma membrane structure, chromatin condensation and fragmentation of DNA by endonucleases [1, 2]. Changes of the plasma membrane structure include a translocation of phosphatidylserine (PS) from the inner leaflet, where it is usually located, to the outer leaflet of the membrane [3] Eukaryotic cells usually maintain an

*Correspondence to: Dr. Carmen SOCACIU,
Department of Chemistry and Biochemistry,
University of Agrcultural Sciences and Veterinary Medicine,
3 Manastur Str., RO-3400, Cluj-Napoca, Romania.
Tel.: 0040 64 196384, Fax: 0040 64 193792.
Email: csocaciu@usamvcluj.ro

asymmetric distribution of phospholipids in their plasma membranes [4, 5, 6]. This process is of essential physiological significance, since the translocated PS serves macrophages to recognize apoptotic cells [7, 8]. The relation of this process with other apoptotic features, particularly DNA fragmentation and cell shrinkage, is still unclear.

The aim of this study was to investigate in more detail the time correlation of changes in plasma membranes, DNA fragmentation and cell shrinkage during apoptosis of EL4 cells which, due to their lymphoma cell origin are considered to be a good model for apoptosis investigations. We relate the time courses of membrane changes and DNA fragmentation and morphological characteristics of the cells are compared. In order to study changes in plasma membrane structure during apoptosis, we investigated the translocation of PS [9, 10], the outer plasma membrane lipids packaging [11] and the plasma membrane fluidity [12].

In our experiments apoptosis of EL4 cells was triggered by three types of inducers: staurosporine (an inhibitor of a wide spectrum of protein kinases), tubercidine (a derivative of adenosine) and x-rays.

This paper intends to contribute to a better understanding of the time courses of apoptotic features, their correlation and the signaling pathways which lead to the execution phase of apoptosis.

Materials and methods

Cell culture

EL4 Cells (European Collection of Cell Cultures (UK)) were cultured in DMEM with 10 % fetal calf serum and 2 mM glutamine, 100 U/ml penicillin and 100 µg/ml streptomycine.

Cultures were incubated at 37°C in humidified air with 5% carbon dioxide, and kept in logarithmic phase by routing passage every 2-3 days. The cells were maintained at a density of 2-9 x 10^5/ml. The isolation of plasma membranes was performed as described [13].

Triggering of apoptosis

Apoptosis was triggered by staurosporine, tubercidine or x-ray irradiation. Cells were suspended in FCS supplemented medium at a density of 5 x 10^5/ml and incubated with the desired concentrations of apoptosis inducers. Solutions of staurosporine (Alexis) 1 mM in DMSO and tubercidine (Sigma) 1 mM in PBS were prepared, then diluted in the medium/serum stock solutions. Dose-response curves for staurosporine (using concentrations from 1 nM up to 10 µM) and tubercidine (using concentrations from 1 nM up to 200 µM) were carried out by methyl triphenyl tetrazolium (MTT, Sigma) assay on a Dynatech well plate reader at 550 nm and the EC_{50} values were determined [14].

Irradiation was performed at a rate of 0.5 Gy/min in a X-ray machine (Mueller RT 100). The irradiated cells were transferred back to culture conditions at a cell density of 5 x 10^5/ml.

Phosphatidylserine translocation

The PS translocation was measured by the annexin V-fluorescein (Boehringer) binding according to the manufacturer instructions. Cells were also stained with 1 µg/ml propidium iodide (PI, Sigma), and analysed with an inverted laser scanning microscope (LSM) (Zeiss 410-488 nm argon laser). Ten pictures were taken and the fluorescence intensities of annexin V-fluorescein and PI for individual cells were determined. Each dot represented a single cell. Volumes of 10 µl cell suspension were analysed, so an average number of 5000 cells was examined. The statistic analysis uses an image processing software. Experiments were performed in triplicate. The results of the ratios of annexin V-positive to annexin V-negative cells were normalized with respect to control cells. Control cells were grown in the same conditions without any addition of apoptosis triggering agents.

Determination of lipid package

3 x 10^6 cells were centrifuged for 5 min at 200g and resuspended in 100 µl merocyanin 540 (MC540, Sigma) solution (5 µg/ml in PBS). A volume of 10 µl of cell suspension was analysed using a Zeiss laser scanning microscope 410 invert by a 543 nm helium neon laser. 10 pictures were taken and the fluorescence intensities of MC540 per cell were determined by an image processing software. Experiments were performed in triplicate. Cells with a decreased lipid package were related to control cells. Control cells were grown in the same conditions without any addition of apoptosis triggering agents.

Determination of plasma membrane fluidity

3 x 10^6 cells were centrifuged 5 min at 200g and resuspended in 3 ml 5 x 10^{-7} M trimethylammonium-diphenylhexatrien (TMA-DPH) (from MoBiTec), in PBS

solution. TMA-DPH was stored as a 0.5 mM stock solution in dimethylformamide. Fluorescence intensity and anisotropy measurements were performed with a Perkin Elmer LS50B.

The sample was illuminated with vertically polarized light (358 +/- 2.5nm) and the components of the emitted intensity respectively polarized vertically ($_{\|}$) and horizontally ($_{\perp}$), with reference to the polarization direction of the excitation light, were measured at

428 +/- 2.5 nm. The stationary fluorescence anisotropy was calculated using the formula:

$r= (I_{\perp} - I_{\|} / I_{\|})+2 I_{\perp}$ [15].

The fluorescence intensities were corrected for scattered light [16].

Determination of DNA fragmentation

8 x 10^6 -10^7cells (control cells or cells treated with apoptotic inducers) were washed in PBS and lysed in 600 µl 10 mM Tris, pH 7.4, containing 3 mM EDTA and 0.2% Triton X-100 for 20 min on ice. Samples were centrifuged for 15 min at 12, 000g at 4°C. The pellet was resuspended in 600 µl of the lysis buffer. The proportion of chromosomal DNA in the pellet and low molecular weight DNA fragments in the supernatant were determined fluorometrically by 4`, 6-diamidino-2-phenylindol (DAPI, MoBiTec), adapting the method rutinely used for the DNA fragmentation [17, 18]. To calibrate the relationship between the content of DNA fragments and the fluorescence intensity, we used aliquots of 5 or 10 µl supernatant which were added five times succesively to a solution containing 100 ng/ml DAPI, 100 mM NaCl, 10 mM EDTA in 10 mM Tris, pH 7.4, and the increase in fluorescence intensity was measured. Fluorescence intensity was proportional to the quantity of fragmented DNA. To measure the DAPI was excited at 362 +/-2.5 nm and the fluorescence was measured at 455+/-2.5 nm by a Kontron SFM Spectrofluorimeter.

Experiments were performed in triplicate and results were normalized with respect to control cells. The internucleosomal DNA fragmentation was confirmed independently from the same samples by gel electrophoresis [19, 20].

Determination of cell size

The size of the cells was determined by an image processing Software recently developed in our group [20]. Single cells were segmented by this routine and the area (number of pixels) of the transmission light picture was evaluated. These area units were used for histograms.

Results

Effect of staurosporine

Staurosporine, which is a streptomyces microbial alkaloid, inhibits PKC by interfering with the ATP binding site. Using staurosporine as an apoptosis inducer, we observed a strong dose-dependent effect on cell viability. The concentration used in experiments was 10 nM (determined previously as EC_{50}, see Materials and methods).

Fig. 1 A-C represents the data obtained from the LSM measurements. The PI uptake due to the breakdown of membrane integrity in late apoptotic or necrotic cells is represented against PS exposure (indicated by the increased annexin V-fluorescein binding). Each dot represented a single cell. The high fluorescence of annexin V - fluorescein indicates the loss of membrane asymmetry. The PI fluorescence indicates its binding to DNA in damaged cells. In Fig.1 A-C, dots in the lower left corner represent normal cells, while dots in the lower right corner represent apoptotic cells. Dots in the upper left corner represent necrotic cells and dots in the upper right corner represent late apoptotic cells. After 3 hours an increase in PS exposure but no significant increase in PI uptake is seen as shown in Fig. 1 B. After 6 hours a loss of membrane integrity was apparent in some cells.

In Fig. 1 D-F the distribution of MC540 labeling is plotted. The histograms show an increase of MC540 binding after 3 and 6 hours of 500 nM staurosporine treatments. This indicates a decrease in lipid package in the outer plasma membrane during apoptosis. The cell size distribution from Fig. 1 G-I shows the apoptotic shrinking process.

In order to examine correlations between the parameters measured, cells were classified in annexin V-positive/negative, increased/not increased MC540 binding and shrunk/not shrunk cells. Additionally the percentage of DNA fragmentation determined by DAPI is shown (Fig. 2). DAPI binds the adenine/thymine clusters in double stranded DNA which lead to increase in its fluorescence intensity about 50 times. After cell lysis and centrifugation, the ratios between the fluorescence of fragmented DNA found in the supernatant and the unfragmented chromosomal DNA represented the apoptotic rate. We checked

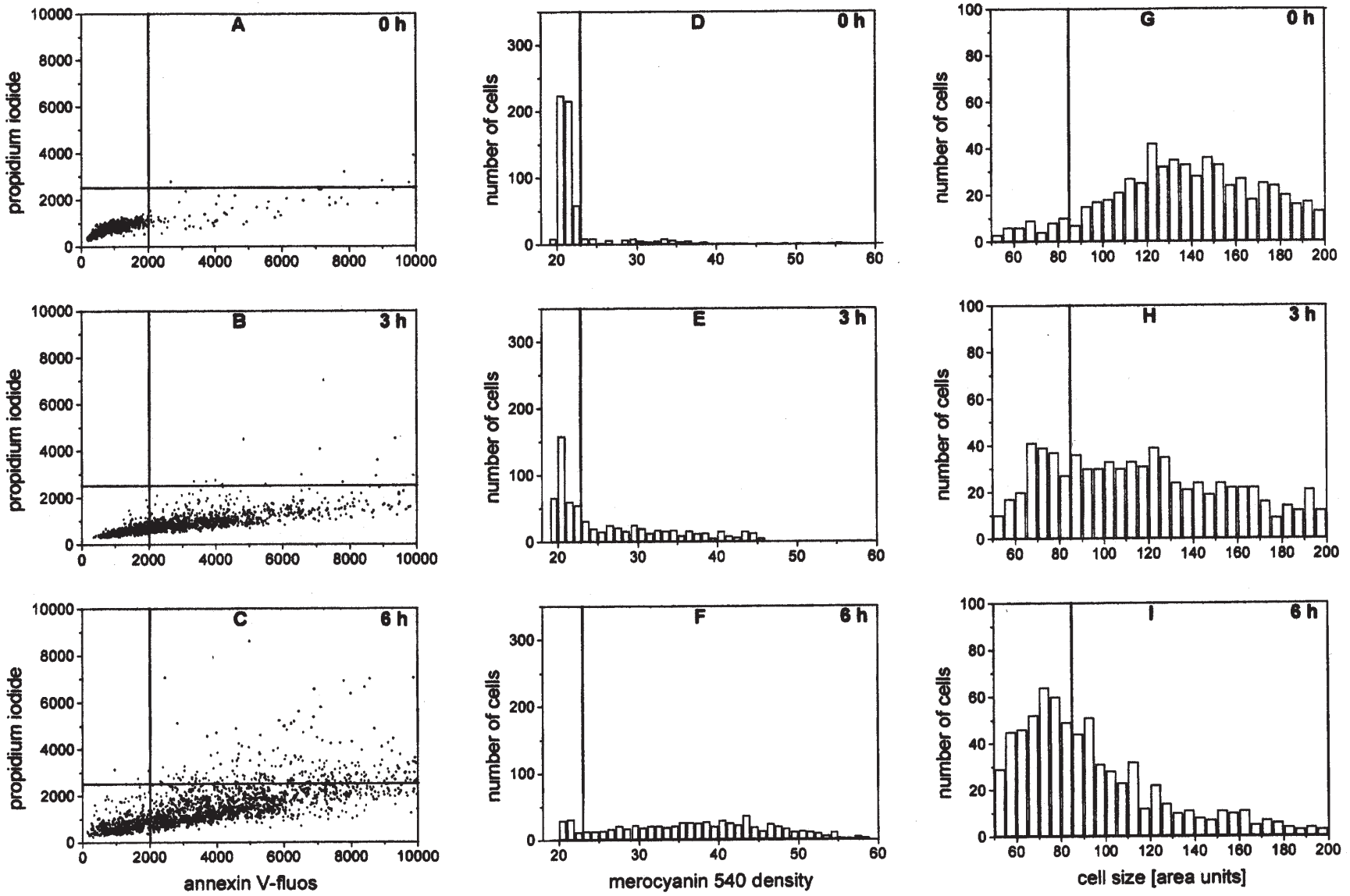

Fig. 1 Histograms of annexin V-fluos binding and propidium iodide permeability (A-C), merocyanin 540 fluorescence density (D-F) and cell size (G-I) after 0 h, 3 h and 6 h of treatment with 500 nM staurosporine, respectively.

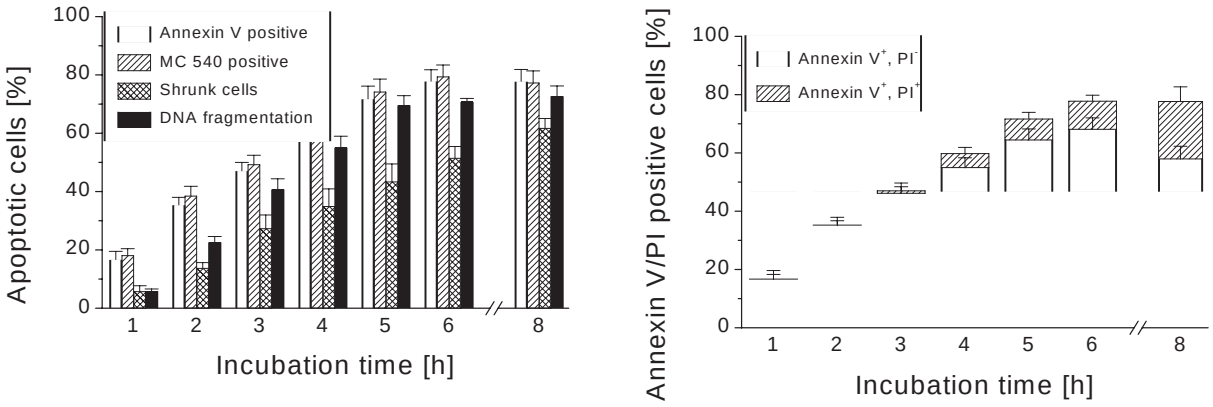

Fig. 2 Percentages of annexin V-positive cells, cells with increased merocyanin 540 binding, shrunk cells and DNA fragmentation after treatment with 500 nM staurosporine. Percentage values were derived from histograms as shown in Fig. 1. Experiments were performed in triplicate. The proportions were normalized with respect to control cells. Values of control cells were in a range between 2 and 5 %. These values were subtracted from values of treated cells.

Fig. 3 Early and late apoptotic cells indicated as annexin V-positive/PI-negative and annexin V-positive/PI-positive after treatment with 500 nM staurosporine. Percentage values were derived from histograms as shown in Fig. 1 A-C. Experiments were performed in triplicate. The proportions were normalized with respect to control cells. Values of control cells were in a range between 2 and 5 %. These values were subtracted from values of treated cells.

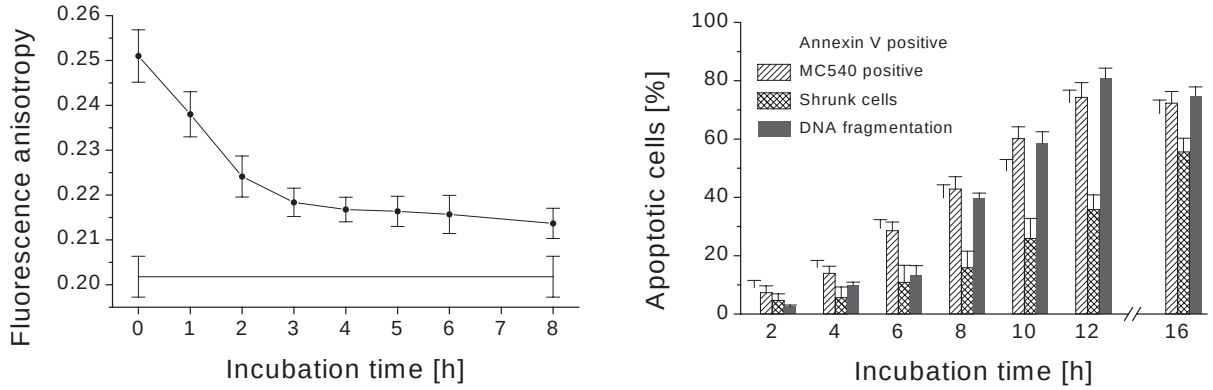

Fig. 4 Fluorescence anisotropy of TMA-DPH in EL4 cells in dependence of the time of incubation with 500 nM staurosporine. Experiments were performed in triplicate. Line graph indicates fluorescence anisotropy of TMA-DPH in isolated plasma membranes of EL4 cells.

Fig. 5 Percentages of annexin V-positive cells, cells with increased merocyanin 540 binding, shrunk cells and DNA fragmentation after treatment with 1 μM tubercidine. Percentage values were derived from histograms. Experiments were performed in triplicate. The proportions were normalized with respect to control cells. Values of control cells were in a range between 2 and 5 %. These values were subtracted from values of treated cells.

these relations by calibration tests, as well by electrophoresis (Comet assay). The kinetics of PS exposure and the decrease of lipid package are similar. Both come up to a plateau after 6 hours. Up to 3 hours the percentages of cells with membrane changes are significantly higher than the percentage of DNA fragmentation. The difference nearly disappeared after 4 hours. This demonstrates the comparatively fast kinetics of lipid asymmetry loss. Cell shrinkage still continues when membrane changes and DNA fragmentation have already come up to a plateau.

The classification of early (annexin V-positive/PI-negative) and late apoptotic cells (annexin V-positive/PI-positive) is shown in Fig. 3. Cells in early apoptosis exclude PI. After about 4 hours the cells which lost membrane integrity become PI positive. This marks the end of the apoptotic process.

Fig. 4 shows the time course of fluorescence anisotropy of TMA-DPH. Due to its positively charged TMA-group, TMA-DPH is located in the outer leaflet of the plasma membrane.

The decrease of anisotropy indicates that fluidity increases in the outer plasma membrane on the same time scale as other membrane changes. The fluorescence anisotropy is compared with isolated plasma membranes of untreated EL4 cells in order to demonstrate the extent of loss of lipid asymmetry. For isolated membranes, a symmetric lipid distribution is supposed and the anisotropy factor r is low and constant (r= 0.202). The difference in fluorescence anisotropy between the apoptotic cell population and the corresponding amount of isolated plasma membranes can be explained by the fact that only about 80% of the cells are apoptotic after 8 hours under 500 nM staurosporine. An extrapolation from 80% to 100% apoptotic cells would result in approximately the same anisotropy value. The conclusion is that the lipid asymmetry is totally lost in apoptotic cells.

Effect of tubercidine

Tubercidine is a derivative of adenosine (substitution of the nitrogen N-7 by a carbon atom). Its EC_{50} concentration was around 200 nM, concentration used to induce apoptosis. Internucleosomal DNA fragmentation was confirmed by gel electrophoresis [20]. The time courses of membrane and cell size changes and of DNA fragmentation are shown in Fig. 5. The kinetics of PS exposure and decrease in lipid packing were similar, leading to the conclusion that both phenomena are based on the same process. DNA fragmentation reached the plasma membrane values only after 6 hours. The time course of cell shrinkage reveals a slower kinetics, a plateau being reached only after 12 hours. Classification of early and late apoptotic cells shows that late apoptotic cells appear after 4 hours, similar to the effect of staurosporine treatment (Fig. 6). The different time course induced by tubercidine in comparison to staurosporine treatment can be explained by its different metabolisation which affect cells in a certain phase or condition. This leads to an asynchronous kinetics of apoptosis (Fig. 7).

To gain more information about the cell cycle dependence of tubercidine induced apoptosis, cells were enriched in the G_1 phase by growing cell up to concentrations of 2 x 10^6 cells/ml. This leads to a nutrient shortage and an accumulation of cells in the G_1 phase. Addition of tubercidine was accompanied by fresh medium bringing the cell density back to the logarithmic phase, so that a normal cell cycle can and a higher percentage of cells enter the S phase.

Figure 8 shows a higher synchronization of apoptosis at 2 and 4 hrs after treatment. This is an indication that tubercidine exerts its effect after cells entered the S phase. Under synchronised conditions the apoptosis rate increased three to six times over the normal rate. DNA fragmentation was more affected than lipid translocations.

Effect of x-rays

Determination of DNA fragmentation under doses of 4, 8 and 12 Gy after 24 and 48 hrs showed a threshold between 4 and 8 Gy in triggering apoptosis (unpublished data). Internucleosomal DNA fragmentation was confirmed by gel electrophoresis [20]. Doses of 4 Gy had nearly no effect but 8 Gy caused a significant increase of apoptotic cells between 24 and 48 hrs, as shown in Fig. 9. The increase of DNA fragmentation, membrane and morphological changes up to 48 hours is remarkable, since the cell cycle time is only

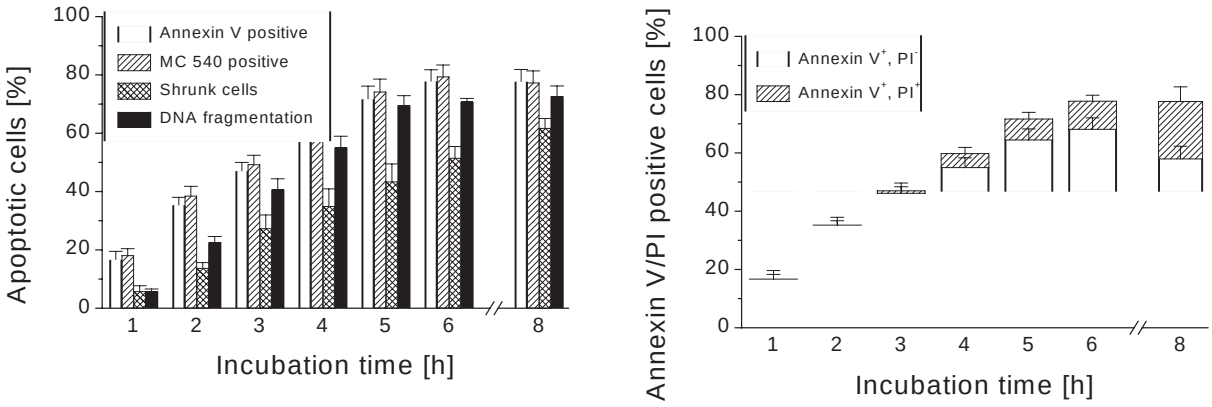

Fig. 6 Early and late apoptotic cells indicated as annexin V-positive/PI-negative and annexin V-positive/PI-positive after treatment with 1 μM tubercidine. Percentage values were derived from histograms. Experiments were performed in triplicate. The proportions were normalized with respect to control cells. Values of control cells were in a range between 2 and 5 %. These values were subtracted from values of treated cells.

Fig. 7 Fluorescence anisotropy of TMA-DPH in EL4 cells in dependence of the time of incubation with 1 μM tubercidine. Experiments were performed in triplicate. Line graph indicates fluorescence anisotropy of TMA-DPH in isolated plasma membranes of EL4 cells.

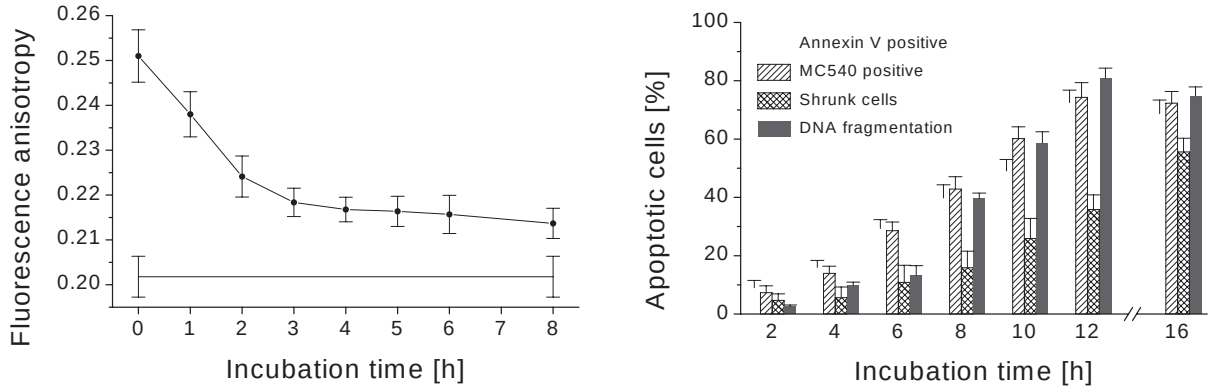

Fig. 8 Apoptosis rates of normal and synchronized EL4 cells indicated by annexin V labeling and DNA fragmentation after treatment with 1 μM tubercidine. Percentage values of annexin positive cells were derived from histograms and of DNA fragmentation by DAPI. Experiments were performed in triplicate.

Fig. 9 Percentages of annexin V-positive cells, cells with increased merocyanine 540 binding, shrunk cells and DNA fragmentation after irradiation with 8 Gy. Percentage values were derived from histograms. Experiments were performed in triplicate. The proportions were normalized with respect to control cells. Values of control cells were in a range between 2 and 5 %. These values were subtracted from values of treated cells.

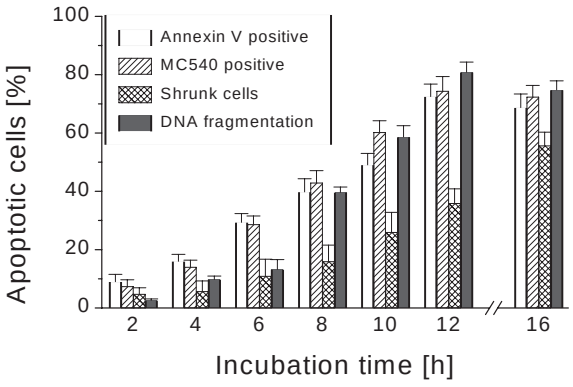

Fig. 10 Early and late apoptotic cells indicated as annexin V-positive/PI-negative and annexin V-positive/PI-positive by irradiation with 8 Gy. Percentage values were derived from histograms. Experiments were performed in triplicate. The proportions were normalized with respect to control cells. Values of control cells were in a range between 2 and 5 %. These values were subtracted from values of treated cells.

about 20 hours. To explain this delay we have to take into account a cell cycle perturbation. Differences between the time courses of the different apoptotic markers were not seen on this time scale. Due to the asynchronic conditions, the proportion of late apoptotic cells was high (Fig. 10).

Discussion

A cascade of intracellular signals determines the passage from normal cells to early- and late-apoptotic cells [1, 21, 22]. The cell susceptibility to undergo apoptosis has been examined with different apoptotic inducers and the consequences for membrane structure and function have been evaluated by different recent studies [3, 7, 22, 23, 24, 25].

Our studies were directed to the time-dependence of apoptotic events at membrane level induced by three different triggers (staurosporine, tubericidine and X-rays). In this study, we examined the phospholipid (PS) translocation, membrane lipid package, membrane fluidity and anisotropy, cell size (shrinkage) and DNA fragmentation. We used EL4 cells – a lymphoma cell line known for its susceptibility to apoptosis [12-19, 23].

Our data show that staurosporine induced a decrease of lipid package observed 4 hrs of treatment, parallel to PS translocation and decrease of membrane anisotropy which were followed by a DNA fragmentation and cell shrinkage effect. By identification of the annexin V-fluorescein positive/PI positive cells we can conclude that early apoptosis is obvious at this time accompanied by the loss of lipid asymmetry.

After tubericidine treatment, the lipid package, membrane asymmetry and PS translocation follow a similar kinetics but DNA fragmentation peaked only after 6 hrs and the time course of cell shrinkage showed an even a slower kinetics. Generally, the tubericidine-induced kinetics is slower, a plateau being reached later (12 hrs), compared to staurosporine (6 hrs). The period of 4 hrs may be considered as a “transition-time” from early to late apoptosis, according to a fixed programme and independent from the trigger.

Contrary to staurosporine, the tubericidine effect was cell-cycle dependent, being more effective in the S-phase of cells. A higher synchronization of apoptosis at 2 and 4 hrs after treatment was observed in this case. The apoptotic rate increased 3-6 times in synchronised S-cells and DNA fragmentation was a more sensible marker for apoptosis than lipid translocations.

When X-rays were used in the appropriate dose-effect range (8Gy), early apoptosis was observed at 12 hrs and late apoptosis continued up to 48 hrs, although EL4 cell cycle time is only 20 hrs. Perturbations of cell cycle by a G2/M arrest can explain this delay. All apoptotic markers followed a similar kinetics. The asynchronic cell cycle phases are responsible for the high rate of late apoptotic cells after 24 hrs.

The similar time courses of the various plasma membrane changes during apoptosis suggest that PS translocation, decrease in membrane lipid package and decrease of membrane anisotropy express the same feature: a translocation of PS from the inner to the outer bilayer leaflet. In unaffected cells the inner leaflet of plasma membranes contains a higher amount of unsaturated fatty acids then the outer leaflet. Phosphatidylcholine and sphingomyeline, located mainly in outer leaflet have highly saturated fatty acids. The PS translocation reverts that to some

extent and it increases the net negative charge of the outer membrane leaflet causing its less dense lipid package. Annexin V as well as merocyanine MC540 and TMA-DPH bind just there. The flip-flop speed cannot be explained only as a diffusion-controlled process because the rate of passive lipid transbilayer diffusion is too slow [26]. So-called scramblases are considered to be responsible for the translocation of aminophospholipids [27, 28], accompanied by a down regulation of an ATP-dependent aminophospholipid translocase, which directs PS to the inner membrane leaflet.

It is worthy to consider how the loss of lipid asymmetry is related to other apoptotic features? The different time courses we found for the loss of lipid asymmetry, the DNA fragmentation and the shrinkage of the cells suggest that they are independent processes with individual kinetics. This is in accordance to the findings of Bratton et al. [29] and Hampton et al.[30] who inhibited PS exposure by removal of extracellular calcium without affecting DNA fragmentation and morphological changes. Van Engeland *et al.* [31] showed an independence of loss of lipid asymmetry and cytokeratin aggregation. The morphological changes of apoptotic cells are subdivided into three phases and are described as to proceed up to 4 hours [32]. It has also been shown that cell nucleus and DNA fragmentation are not always required for apoptosis [33]. Caspases are discussed to play a key role in initiating apoptosis [28, 34] and a breakdown of mitochondrial membrane potential was found to occur prior to PS exposure [31].

It can be concluded that PS translocation and DNA fragmentation are characteristic but not necessary processes of apoptosis. We show that loss of lipid asymmetry is faster than DNA fragmentation and cell shrinkage. The cell shrinkage is the slowest of these processes. The membrane changes are parallel processes and provide an early indication of apoptosis.

Staurosporine and tubericidine triggered apoptosis on a different extent of synchronism in the cell population. Asynchronous death is a characteristic feature of apoptosis, in many cases about 5-10% of cells are in the execution phase of apoptosis [35]. A balance of different antagonistic protein kinase activities may explain it [36].

The parameters indicating apoptosis caused by tubercidine all run on a longer time scale than those caused by staurosporine. The modes of action of tubercidine are not completely clear, but it has been postulated that the antitumoral action of tubercidine relies in its incorporation into DNA and RNA through the purine metabolism [35]. Incorporation of tubercidine into the DNA can occur in the S phase only, when modifications of DNA structure may lead to apoptosis.

Our results showed that it is very likely that the induction of apoptosis by tubercidine occurs only in the S phase and is connected to an incorporation into the DNA. Usually the S phase takes 30% of the time of a complete cell cycle, but the cell cycle of EL4 takes approximately 20 hours. The appearance of apoptotic cells increased until up to 12 hours. This could approximately be brought to accordance with an apoptosis induction in the S phase of the cell cycle, it means that cells have to enter the S phase before tubercidine can trigger apoptosis by incorporation in the DNA. Confirmation was achieved by the performance of a synchronisation procedure, where an accumulation of EL4 cells in the G_1 phase is provoked via nutrient shortage. If those cells were brought back into in the logarithmic phase by adding fresh medium/serum, they re-enter into the S phase at a considerable higher number. The significant higher rates of apoptosis checked after 2 and 4 hours of synchronisation, each, confirmed the hypothesis.

X-rays imposed the slowest time course of apoptotic features. The apoptotic kinetics extended over a much longer period than a normal cell cycle. This can be explained by a cell cycle arrest ending either by repair or apoptosis, as it was observed in EL4 cells where a G_2/M block after ionizing radiation was found [37]. Both processes depend on dose and post-irradiation time. Apoptosis appeared after a period of delay of the progression of cells in the cell cycle. Such an arrest may take place at different points in the cell cycle. Exposure to radiation induced a more pronounced G_2/M block, and in those cases apoptosis appeared to be manifest at the time of cells release from the G_2/M block, during the subsequent G_1 phase [38, 39].

In conclusion, the plasma membrane changes, the DNA fragmentation and the shrinkage of the cells seem not to be downstream events but parallel processes running on different time scales, but kinetically inter-related.

References

1. **Kerr J. F. R., Wyllie, A. H., Currie, A, R.,** Apoptosis: a basic biological phenomenon with wide-ranging implications in tissue kinetics, *Br. J. Cancer,* 26: 239-257, 1972
2. **Arends M. J., Morris R. G., Wyllie A. H.,** Apoptosis. The role of the endonuclease, *Am. J. Pathol.*, 136: 593-608, 1990
3. **Denecker G., . Dooms H, Van Loo G., Vercammen D., Grooten J., Fiers W., Declercq W. and Vandenabeele P**., Phosphatidyl serine exposure during apoptosis precedes release of cytochrome c and decrease in mitochondrial transmembrane potential, FEB*S Lett.*, 465: 47-52, 2000.
4. **Devaux P. F.,** Protein involvement in transmembrane lipid asymmetry, *Ann. Rev. Biophys. Biomol. Struct.*, 21: 417-439, 1992.
5. **Devaux P. F**., Lipid transmembrane asymmetry and flip-flop in biological membranes and in lipid bilayers, *Curr. Opinion Struct. Biol.*, 3: 489-494, 1993
6. **Op den Kamp J. A. F.,** Lipid asymmetry in membranes, *Ann. Rev. Biochem.*, 48: 47-71, 1979
7. **Kagana V. E., Fabisiaka J. P., Shvedovad A. A., Tyurinaa Y. Y., 1, Tyurina V. A., Schorb N. F., and Kawaia K.,** Oxidative signaling pathway for externalization of plasma membrane phosphatidylserine during apoptosis, *FEBS Lett.*, 477: 1-7, 2000
8. **Shiratsuchi A., Osada S., Kanazawa S., Nakanishi Y.,** Essential role of phosphatidylserine externalization in apoptosing cell phagocytosis by macrophages, *Biochem. Biophys. Res. Comm.*, 246: 549-555, 1998
9. **Andree H. A., Reutelingsperger C. P., Hauptmann R., Hemker H. C., Hermens W. T., Willems G. M.,** Binding of vascular anticoagulant alpha (VAC alpha) to planar phospholipid bilayers, *J. Biol. Chem*., 265: 4923-4928, 1990
10. **Thiagarajan P., Tait J. F.,** Binding of annexin V/placental anticoagulant protein I to platelets. Evidence for phosphatidylserine exposure in the procoagulant response of activated platelets, *J. Biol. Chem*., 265: 17420-17423, 1990
11. **Ashman R. F., Peckham D., Alhasan S., Stunz L. L.,** Membrane unpacking and the rapid disposal of apoptotic cells, *Immunol. Lett.*, 48: 159-166, 1995
12. **Kuhry J.-G., Duportail G., Bronner C., Laustriat G,** Plasma membrane fluidity measurements on whole living cells by fluorescence anisotropy of trimethylammoniumdiphenylhexatriene, *Biochim. Biophy. Acta*, 845: 60-67, 1985
13. **Evans W. H.,** Preparation and characterization of lymphocyte plasma membranes, *Laboratory Techniques in Biochemistry and Molecular Biology,* 7:32-45, 1979.
14. **Mosmann T.,** Rapid colorimetric assay for cellular growth and survival: application to proliferation and cytotoxicity assays, *J. Immunol. Meth.*, 65: 55-61, 1983
15. **Shinitzky M., Barenholz Y.,** Fluidity parameters of lipid regions determined by fluorescence polarization, *Biochim. Biophys. Acta,* 515: 367-394 1978
16. **Lentz B. R., Moore B. M., Barrow D. A.,** Light scattering effects in the measurement of membrane microviscosity with diphenylhexatriene, *Biophys. J.*, 25: 489-494, 1979
17. **Kapuscinski J.,** DAPI: A DNA-specific fluorescent probe, *Biotech. Histochem.*, 70, 220-233, 1995
18. **Masotti L., Cavatorta P., Avitabile M., Barcellona M. L., von Berger J., Ragusa N.,** Characterization of 4'-6 diamidino-2 phenylindole (DAPI) as a fluorescent probe of DNA structure, *Italian J. Biochem.*, 31: 90-99, 1982
19. **Hinshaw V. S., Olsen C. W., Dybdahl-Sissoko N., Evans D.,** A mechanism of cell killing by influenza A and B viruses, *J. Virology,* 68: 3667-3673, 1994
20. **Haertel S.,** Quantifizierung von Strukturen, Kinetik und Dynamik nekrobiologischer Prozesse mit Hilfe bildverarbeitender konfokaler Fluoreszenzmikroscopie, PhD Diss, University of Bremen, Germany, 2000.
21. **Schwartzman R. A., Cidlowski J. A.,** Apoptosis: The biochemistry and molecular biology of programmed cell death, *Endocrine Rev.*, 14: 133-151, 1993
22. **Pothana S., Dong Z., Mikhailov V., Denton M., Weinberg J.M. and Venkatachalam M.A.,** Apoptosis: definition, mechanisms, and relevance to disease, *Am.J. Med.*, 107, 489-506, 1999.
23. **Nielson KH, Olsen CA, Allred DV, O'Neill KL, Burton GF, Bell JD,** Susceptibility of S49 lymphoma cell membranes to hydrolysis by secretory phospholipase A(2) during early phase of apoptosis, *Biochim. Biophys. Acta*, 1484:163-74, 2000.
24. **Albanese J, Dainiak N.,** Ionizing radiation alters Fas antigen ligand at the cell surface and on exfoliated plasma membrane-derived vesicles: implications for apoptosis and intercellular signaling, *Radiat. Res*., 153:49-61, 2000.
25. **Matés J. M., and Sánchez-Jiménez F.M.,** Role of reactive oxygen species in apoptosis: implications for cancer therapy, *Int. J. Biochem. & Cell Biol.*, 32: 157-170, 2000.

26. **Pervaiz S., Hirpara J. L., Clément M.-V.,** Caspase proteases mediate apoptosis induced by anticancer agent preactivated MC540 in human tumor cell lines, *Cancer Lett.*, 128: 11-22, 1998.
27. **Smeets E. F., Comfurius P., Bevers E. M., Zwaal R. F. A.,** Calcium-induced transbilayer scrambling of fluorescent phospholipid analogs in platelets and erythrocytes.}\\
Biochim. Biophys. Acta, 1195: 281-286, 1994
28. **Williamson P., Kulick A., Zachowski A., Schlegel R. A., Devaux P. F.,** Ca $^{2+}$ induces transbilayer redistribution of all major phospholipids in human erythrocytes, *Biochemistry*, 31: 6355-6360, 1992.
29. **Bratton D. L., Fadok V. A., Richter D. A., Kailey J. M., Guthrie L. A., Henson P. M.,** Appearance of phosphatidylserine on apoptotic cells requires calcium-mediated nonspecific flip-flop and is enhanced by loss of the aminophospholipid translocase, *J. Biol.Chem.*, 272: 26159-26165, 1997.
30. **Hampton M. B., Vanags D. M., Poern-Ares I., Orrenius S.,** Involvement of extracellular calcium in phosphatidylserine exposure during apoptosis, *FEBS Lett.*, 399: 277-282, 1996.
31. **van Engeland M., Kuijpers H. J. H., Ramaekers F. C. S., Reutelingsperger C. P. M., Schutte B.,** Plasma membrane alterations and cytosceletal changes in apoptosis, *Exp.Cell Res.*, 235: 421-430, 1997
32. **Messam C. A., Pittman R. N.,** Asynchrony an commitment to die during apoptosis, *Exp.Cell Res.*, 238: 389-398, 1998
33. **Jacobson M. D., Weil M., Raff M. C.,** Role of Ced-3/ICE-family proteases in staurosporine-induced programmed cell death, *J. Cell Biol.*, 133: 1041-1051, 1996
34. **Rudel T., Bokoch G.M.,** Membrane and morphological changes in apoptotic cells regulated by caspase-mediated activation of PAK2, *Science*, 276: 1571-1574, 1997.
35. **Ojeda F., Folch H., Guarda M. I., Jastorff B., Diehl H.A.,** Induction of apoptosis in thymocytes: New evidence for an interaction of PKC and PKA pathways, Biol.Chem. Hoppe-Seyler 376: 389-393, 1995
36. **Bloch A., Leonard R. J., Nichol C. A.,** On the mode of action of 7-deaza-adenosine. *Biochim.Biophys. Acta*, 138: 10-25, 1967
37. **Palayoor S. T., Macklis R. M., Bump E. A., Coleman C. N,** Modulation of radiation-induced apoptosis and G/M block in murine T-lymphoma cells, *Radiat. Res.*, 141: 235-243, 1995
38. **Kruman I. A., Matylevich N. P., Beletsky I. P., Afanasyev V. N., Umansky S. R.,** Apoptosis of murine BW 5147 thymoma cells induced by dexamethasone and γ–irradiation, *J. Cell Physiol.*, 148: 267-273, 1991
39. **Radford I. R., Murphy T. K.,** Radiation response of mouse lymphoid and myeloid cell lines. Part3. Different signals can lead to apoptosis and may influence sensitivity to killing by DNA double strand breakage, *Int. J. Radiat.Biol.*, 65: 229-239, 1994